Available online at www.sciencedirect.com
SCIENCE DIRECT
Energy Conversion and Management 47 (2006) 1311–1325
ENERGY CONVERSION & MANAGEMENT
www.elsevier.com/locate/enconman

Flow and heat transfer in microchannels with rough wall surface

S. Shen, J.L. Xu *, J.J. Zhou, Y. Chen

Guangzhou Institute of Energy Conversion, Micro Energy System Laboratory, Chinese Academy of Sciences, Nengyuan Road, Wushan, Guangzhou, Guangdong 510640, PR China

Received 25 August 2004; received in revised form 1 March 2005; accepted 11 September 2005
Available online 19 October 2005

Abstract

Experiments were conducted to investigate the single phase convective heat transfer in a compact heat sink consisting of 26 rectangular microchannels of 300 μm width and 800 μm depth. The relative roughness is estimated to be 4–6%. Deionized water was used as the working fluid. Tests were performed with the Reynolds number range of 162–1257, the inlet liquid temperatures of 30, 50 and 70 °C and the heating powers of 140–450 W. The planform area is 5.0×1.53 cm^2. It is found that the friction factors and local and average Nusselt numbers significantly depart from those of conventional theories, possibly attributable to the surface roughness. The hydraulically developed but thermally developing flow results in decreased Nusselt numbers versus the non-dimensional axial distance. The temperature dependent fluid physical properties also influence the heat transfer characteristics to some extent. Correlations were provided for the friction factors and the Nusselt numbers.

Keywords: Microchannels; Surface roughness; Thermally developing flow; Heat transfer

1. Introduction

Nowadays, it is possible to develop various microdevices or systems such as microchannel heat sinks, micropumps, microreactors, microvalves and microactuators. Understanding the flow and heat transfer in microscale is useful for the design, fabrication and operation of these microdevices or systems.

Many studies have been conducted for single phase convective heat transfer in microchannels. It is demonstrated that some results significantly deviate from conventional theory, which is well established for macrosize. A literature survey shows that the available results are often conflicting, partially due to measurement errors and fabrication methods. A lot of factors influence the experimental results, including the surface roughness of the microchannels, temperature dependent physical properties, surface physical effects and so on. At this stage, it is still uncertain as to the true factors that affect the flow and heat transfer behaviors in microscale.

* Corresponding author. Tel./fax: +86 20 87057656.
E-mail address: xujl@ms.giec.ac.cn (J.L. Xu).

0196-8904/$ - see front matter © 2005 Elsevier Ltd. All rights reserved.
doi:10.1016/j.enconman.2005.09.001

Nomenclature

A_c	cross-section area of one microchannel, m^2
C_p	specific heat, J/kg °C
D_h	hydraulic diameter of microchannel, m
f	Darcy friction factor
H_{w1}	thickness of glass cover plate, m
H_{w2}	height from bottom wall to locations where thermocouple wires are located, m
H_{ch}	height of microchannel, m
h	heat transfer coefficient, W/m^2 K
k	channel surface roughness, m
k/D_h	surface relative roughness
k_c	entrance pressure loss coefficient
k_e	exit pressure loss coefficient
L	channel length, m
L^+	non-dimensional channel flow length
L_h^+	non-dimensional channel heating length
L_E	entrance length, m
l_{min}	shortest distance from point to surface of microchannel, m
M	mass flow rate, kg/s
m	fin parameter
N	total number of microchannels
Nu_x	local Nusselt number
Nu	averaged Nusselt number
Δp	pressure drop over microchannels, Pa
Pr	Prandtl number
q	effective heat flux, W/m^2
Q	effective heating power, W
R	thermal resistance, °C/W
Re	Reynolds number
Re_{eff}	effective Reynolds number
T_c	temperature measured by thermocouples, °C
T_f	fluid temperature, °C
T_{in}	inlet fluid temperature, °C
ΔT_m	mean temperature difference, °C
T_{out}	outlet fluid temperature, °C
T_w	bottom wall temperature, °C
u	fluid velocity, m/s
W_{ch}	width of microchannel, m
W_w	half width between neighboring microchannels, m
X	axial distance from channel entrance, m
X^+	non-dimensional axial distance
γ	channel aspect ratio
λ_f	liquid thermal conductivity, W/m K
λ_s	solid copper thermal conductivity, W/m K
η	fin efficiency
μ_{eff}	effective viscosity, Pa s
μ_f	fluid viscosity, Pa s
μ_R	roughness viscosity, Pa s
ρ	liquid density, kg/m^3
τ_w	wall shear stress, Pa

Using the conventional precision machining method, the surface roughness is an important factor affecting the flow and heat transfer in microchannels. Wu and Little [1] measured the friction factors for silicon and glass capillary tubes using gases (N_2, H_2, Ar) as the working fluids. The measured friction factors were 10–30% higher than the conventional theory predictions. Furthermore, the critical Reynolds numbers at which the laminar flow transitions to turbulent flow for such test sections is between 350 and 900, which is attributed to the channel surface roughness. Later, Wu and Little [2] reported the Nusselt numbers in counter-flow heat exchangers for which the microchannels were 312–572 μm wide and 89–97 μm deep. For fully developed laminar flow, the Nusselt numbers oscillated greatly with Reynolds numbers. In the turbulent regime, the Nusselt numbers were higher than the conventional theory predictions. They attributed such deviations to the asymmetric wall roughness and the uneven wall heating.

Experiments were performed by Kandliker et al. [3] to study the effect of the relative roughness on the pressure drop and heat transfer in two capillary tubes with diameters of 1076 μm and 600 μm with relative roughness ranging from 0.00178 to 0.003. It was observed that the effect of the relative roughness on the pressure drop can be neglected, and thus, the 1076 μm microtube can be considered smooth. The measured local Nusselt numbers agreed with conventional theory well, but for the microtube with the diameter of 620 μm, the higher relative roughness increased the friction factors and the Nusselt numbers. Thus, one can see that the wall roughness can play a more important role in microchannels than that in macrochannels.

There are a lot of wall roughness definitions, and thus, it is difficult to quantify the effect of wall roughness on the flow and heat transfer in microchannels at this stage. Such effects could be quantified by experiment and numerical modeling. Qu et al. [4] measured the water flow in trapezoidal silicon microchannels with hydraulic diameters ranging from 51 to 169 μm. The measured friction factors were higher than the conventional theory predictions in the laminar flow regime. In terms of the eddy viscosity concept for turbulent flow, they proposed a roughness-viscosity model to explain the discrepancy between the measured friction factors and the conventional theory predictions. Qu et al. [5] measured the heat transfer coefficients for water flowing through trapezoidal silicon microchannels with hydraulic diameters ranging from 62 to 169 μm. The measured values were compared with numerical predictions with coupling the heat transfer in the solid and the fluid regions. They found that the measured Nusselt numbers are much lower than those of the numerical solutions. The numerical solutions based on their improved numerical model agree with their experimental data well.

The objective of this paper is to study the liquid flow and heat transfer in rough copper microchannels. The early transition from laminar to turbulent flow reported in previous studies was not observed in the present study. The hydraulic flow was considered as laminar flow. The effect of surface roughness was highlighted and evaluated in comparison with the effects predicted by conventional theory. A detailed description of the friction factors and local and average heat transfer coefficients is presented and discussed, considering the effects of inlet fluid temperatures and heating powers. Also, the effects of the hydraulic and thermal boundary layer growth on the experimental results are emphasized, which were neglected in previous studies.

2. Experimental setup

Fig. 1 shows the experimental setup. Deionized water was pumped from a liquid reservoir to the test section through a 15 μm filter, preventing any solid particles from entering the microchannels. An electronic heater was immersed in the liquid tank with a proportional-integral-derivative (PID) temperature control unit to obtain any desired liquid temperature. The flow rate was obtained by adjusting the valve located in the bypass line and the throttling valve upstream of the microchannel test section. One of two water flow meters was selected based on the flow rate. The flow meters were calibrated by weighing the outlet liquid over a given period of time using an electronic balance with an accuracy of 0.01 g.

Jacket thermocouples were used to measure the inlet and outlet fluid temperatures. These thermocouples have an accuracy of 0.5 °C and a response time of 50 ms. A Setra pressure transducer (Model 206) was used to measure the inlet fluid pressure. The uncertainty of the pressure transducer was less than 0.1% after calibration with a known standard. The pressure drop over the microchannel test section was measured by a Senex differential pressure transducer with an accuracy of 0.1% and a response time of 10 ms. A HP high speed data acquisition system was used to collect all the temperatures, pressure and differential pressure drop signals. The data was displayed by a PC monitor and stored in PC memory for further analysis.

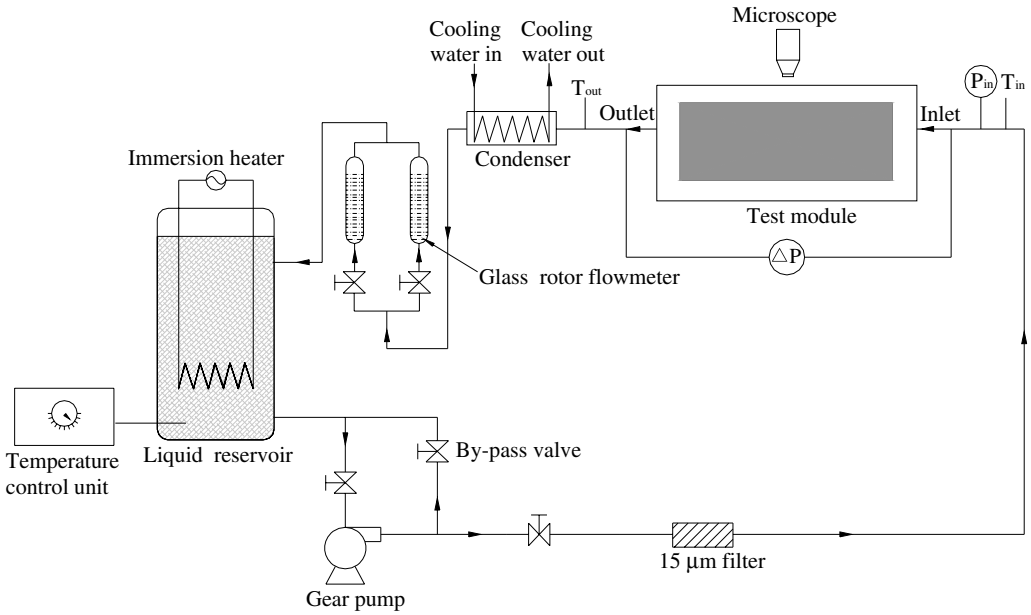

Fig. 1. Experimental test loop.

Figs. 2 and 3 illustrate the three-dimensional view and the detailed technical drawing of the microchannel heat sink, respectively. The microchannel heat sink component has an O-ring slot, a glass cover plate and a

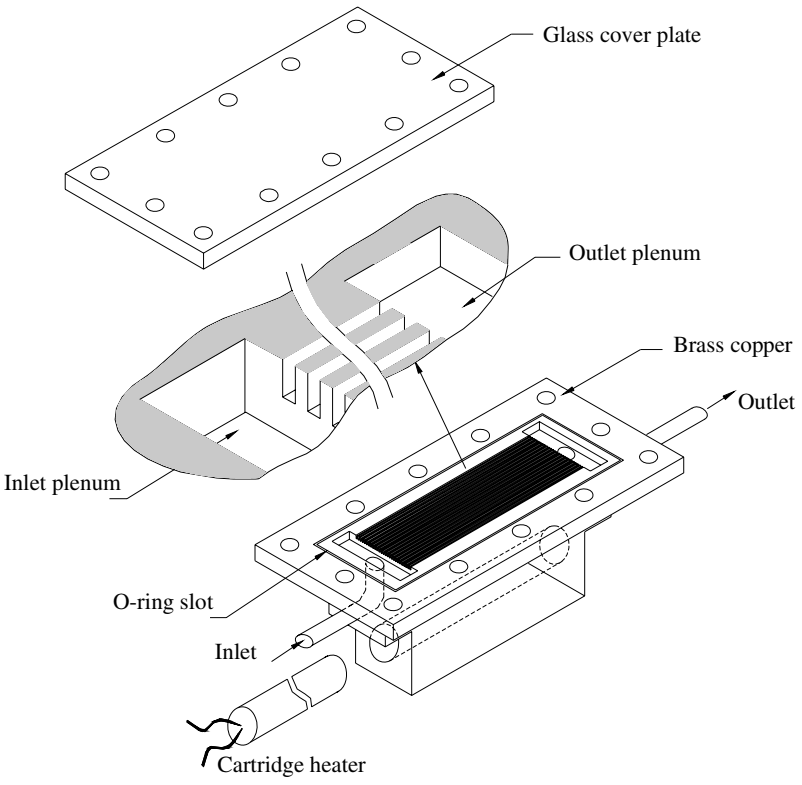

Fig. 2. Three-dimensional view of the copper heat sink.

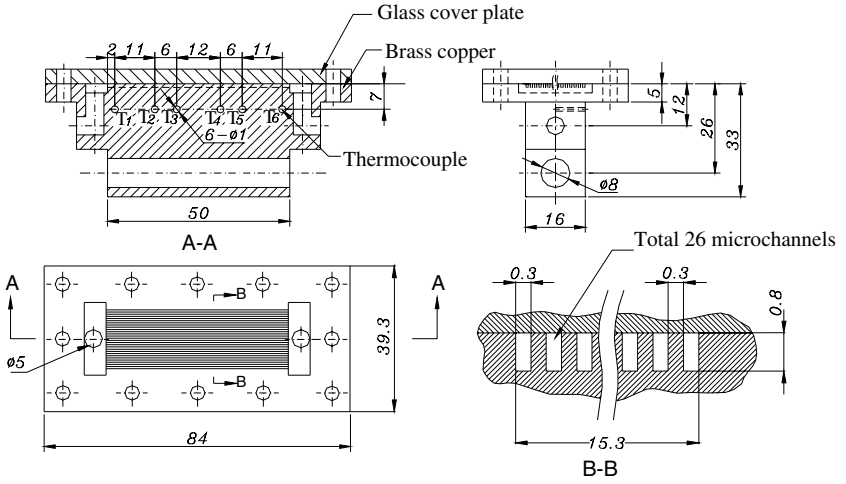

Fig. 3. Detailed technical drawing of the copper microchannel heat sink.

cartridge heater. There are 26 microchannels with 300 μm width and 800 μm depth. The microchannels were made in the copper block using a micromachining technique. The relative wall roughness k/D_h was estimated to be 4% by microscope. The planform (top) surface of the heat sink was 1.53 cm wide and 5.0 cm long. There is a hole with the diameter of 8.0 mm in the copper block to accommodate the cartridge heater, and the heating power was measured by a precision wattmeter with an accuracy of 0.5%. Below the heat sink is the six K-type thermocouples to measure the axial temperature distribution along the flow direction, whose locations are shown in Fig. 3.

A cover plate made from transparent plastic (Lexan) was bonded with the copper heat sink. An O-ring slot was machined in the top surface of the microchannel heat sink, preventing any leakage from the microchannel slots.

The experiments were performed with inlet liquid temperatures of 30, 50 and 70 °C, mass fluxes of 20–1200 kg/m^2 s and effective heating powers of 140–450 W.

3. Data reduction

Before performing the data reduction, the following assumptions are made: (1) Each parallel microchannel has exactly the same size and wall roughness. (2) Flow rates in each microchannel are the same. (3) The conduction heat transfer in the solid copper block is one-dimensional in the height direction. Heat conduction in the solid copper block along the flow direction is neglected. (4) The heat flux for each microchannel is the same.

3.1. Flow friction

The Darcy friction factor f can be deduced from the pressure drop of the fluid flowing through the microchannels.

$$f = \frac{8\tau_w}{\rho u^2} = \frac{2D_h \Delta p}{\rho u^2 L} \tag{1}$$

where Δp is the pressure drop over the microchannels and ρ is the fluid density. The mean liquid temperature in terms of the inlet and outlet values characterize the fluid properties, such as thermal conductivity λ, viscosity μ and specific heat C_p. D_h and L are the hydraulic diameter and the length of the microchannels, and u is the average liquid velocity obtained by

$$u = \frac{M}{N\rho A_c} \tag{2}$$

where M is the liquid mass flow rate, N is the number of microchannels and A_c is the cross-sectional area of a single microchannel.

Note that the measured pressure drop includes the entrance and exit pressure losses due to the sharp change of cross-section area. Therefore, the net friction pressure drop over the microchannels is calculated as

$$\Delta p = \Delta p_{\text{measured}} - (k_c + k_e)\frac{\rho u^2}{2} \tag{3}$$

where k_c and k_e are the entrance and exit pressure loss coefficients, and can be estimated from Kays and London [6].

The Reynolds number is defined as

$$Re = \frac{\rho u D_h}{\mu_f} \tag{4}$$

where μ_f is the liquid viscosity based on the mean fluid temperature. The Poiseuille number fRe is defined as the product of the friction factor and the Reynolds number.

3.2. Heat transfer

To compute the heat transfer coefficient for deionized water flowing through the microchannels, a two-dimensional unit cell consisting of a single microchannel and the surrounding solid is identified along the flow direction where the thermocouple wires are located. The two-dimensional unit cell is shown in Fig. 4, and the geometric parameters are listed in Table 1. The heat transfer coefficient can be acquired from the fin analysis method used by Harms et al. [7].

The energy conservation equation of the unit cell is given by

$$qW_{\text{cell}} = h(T_w - T_f)(W_{ch} + 2\eta H_{ch}) \tag{5}$$

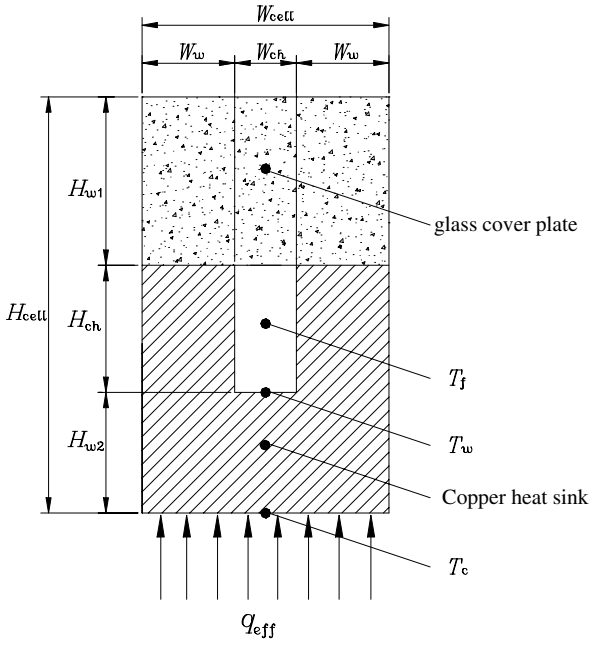

Fig. 4. Two-dimensional microchannel heat sink unit cell.

Table 1
Geometric parameters of unit cell

W_w (μm)	W_{ch} (μm)	H_{w1} (μm)	H_{ch} (μm)	H_{w2} (μm)
150	300	5000	800	6200

The left hand side of Eq. (5) is the heat input to the unit cell, and the right hand side is the heat dissipated by the fluid. The fin efficiency η is computed as

$$\eta = \frac{\tanh(mH_{ch})}{mH_{ch}} \tag{6}$$

The fin parameter m in Eq. (6) is defined as

$$m = \sqrt{\frac{h}{\lambda_s W_w}} \tag{7}$$

where λ_s is the thermal conductivity of the solid copper block. A linear liquid temperature distribution along the flow direction is assumed, based on the inlet and outlet liquid temperatures.

$$T_f = T_{in} + \frac{X}{L}(T_{out} - T_{in}) \tag{8}$$

where X is the axial distance from the channel entrance. The microchannel bottom wall temperature T_w is evaluated using the one-dimensional heat conduction equation as

$$T_w = T_c - \frac{qH_{w2}}{\lambda_s} \tag{9}$$

where T_c is the temperature measured by the thermocouples.

The Nusselt number based on the heat transfer coefficient is given by

$$Nu = \frac{hD_h}{\lambda_f} \tag{10}$$

where λ_f is the liquid thermal conductivity.

The thermal resistance of the microchannel system is defined as

$$R = \frac{\Delta T_m}{q} \tag{11}$$

where ΔT_m is the mean temperature difference evaluated by

$$\Delta T_m = (T_{c1} + T_{c2} + T_{c3} + T_{c4} + T_{c5} + T_{c6})/6 - (T_{in} + T_{out})/2 \tag{12}$$

where $T_{c1}, T_{c2}, \ldots, T_{c6}$ are the temperatures measured by the six thermocouples.

3.3. Uncertainty analysis

The errors of the friction factors and Nusselt numbers come from the measurement errors of a set of parameters. Performing the standard error analysis, the maximum uncertainties in determining these parameters are given in Table 2. It is seen that the maximum errors due to the measurements are less than 7.1% and 5.93% for f and Nu, respectively. Even though all the temperatures measured by the thermocouples are carefully calibrated, the maximum errors of 0.5 °C are used for the analysis. Normalizing such error with respect to the minimum inlet liquid temperature yields the maximum possible error of 1.67% for the temperatures.

Table 2
Measured and deduced parameter errors

Parameters	Maximum errors (%)
D_h	4
L	0.12
L_h	0.12
W_{ch}	4
H_{ch}	4
M	1.02
Δp	0.1
T	1.67
ΔT_m	1.67
Re	6.95
f	7.1
Nu	5.93

4. Results and discussion

4.1. Flow friction

The conventional theory based on the Navier–Stokes equation for fully developed laminar flow through rectangular microchannels indicates that the Poiseuille number can be calculated as follows,

$$f\,Re = C(\gamma) \tag{13}$$

where the constant C only depends on the rectangular aspect ratio γ. Morini [8] calculated the values of C for three different cross-section channels: rectangular, trapezoidal and double trapezoidal. For the microchannels used in our experiment ($\gamma = 0.375$), the constant C equals 67, which can be considered as the theoretical prediction to be compared with the experimental results.

To identify the effect of the hydraulic entrance region on the flow resistance, the non-dimensional axial distance is defined as

$$L^+ = \frac{L}{D_h Re} \tag{14}$$

Fig. 5 illustrates the measured $f\,Re$ versus the non-dimensional channel length L^+. Now, we turn to consider the rough microchannels characterized as k/D_h within the range of 4–6%. Generally, the presence of the surface roughness enhances the momentum transfer near the wall. Such effect is approximately equivalent to an increase in the fluid viscosity [4,5]. An effective viscosity μ_{eff} in rough microchannels can be defined as the fluid

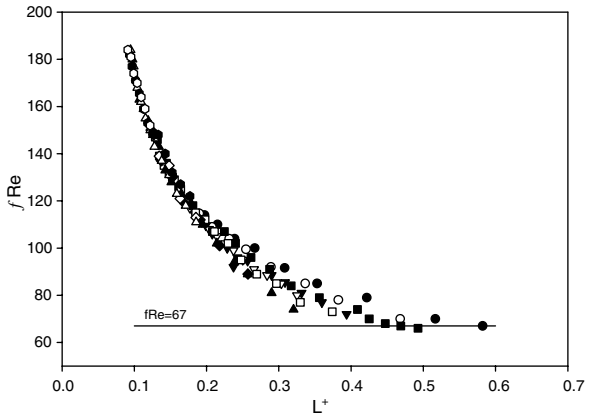

Fig. 5. The Poiseuille number $f\,Re$ versus the non-dimensional microchannel flow length L^+.

viscosity μ_f plus the additional roughness-viscosity μ_R. μ_R should have higher values near the wall and gradually diminish toward the channel center area. Also, μ_R should be proportional to Re and k/D_h [9]. The roughness-viscosity μ_R can be described in terms of $\mu_R = f(Re, k/D_h, l_{min})$, where l_{min} is the shortest distance from the examined point to the microchannel surface.

Consider the effect of the hydraulic developing laminar flow where the entrance length L_E [10] is given by

$$L_E = 0.065 D_h \frac{\rho u D_h}{\mu} \tag{15}$$

Eq. (15) shows that the increase of the fluid viscosity leads to a shorter entrance length. Therefore, compared with smooth microchannels, the entrance effect in rough microchannels is weakened for the given inlet fluid velocity and geometric parameters. For conventional, smooth microchannels, the entrance effect is found to be negligible when L^+ is higher than about 0.1 [11]. In other words, flow in smooth microchannels is fully developed for $L^+ > 0.1$. It is interesting to note that all our experimental data drop in the regime of $L^+ > 0.1$. For the given inlet fluid velocity and channel geometric parameters, the entrance effect in the present study is negligible compared to that in smooth microchannels when $L^+ > 0.1$. Apparently, the flow in the present microchannels should be fully developed. So, the inverse relationship between fRe and L^+ in Fig. 5 is not due to the developing laminar flow.

The inverse relationship between fRe and L^+ may be explained by the high surface roughness of the microchannels. Assuming that the effect of l_{min} on the roughness-viscosity μ_R can be neglected, μ_R is only a function of Re and k/D_h. The friction factor for developed flow through smooth microchannels can be calculated by

$$fRe = 67 \tag{16}$$

For the given inlet fluid velocity or Re and the surface relative roughness k/D_h, the friction factor in rough microchannels yields

$$fRe_{eff} = 67 \tag{17}$$

where the effective Reynolds number is defined as

$$Re_{eff} = \frac{\rho u D_h}{\mu_{eff}} = \frac{\rho u D_h}{\mu_f + \mu_R} \tag{18}$$

Substituting Eq. (18) into Eq. (17) provides

$$\begin{aligned} f\frac{\rho u D_h}{\mu_f + \mu_R} &= 67 \\ f\frac{\rho u D_h}{\mu_f} \cdot \frac{\mu_f}{\mu_f + \mu_R} &= 67 \\ fRe = 67\frac{\mu_f + \mu_R}{\mu_f} &= 67\left[1 + \frac{\mu_R(Re, k/D_h)}{\mu_f}\right] \end{aligned} \tag{19}$$

Eq. (19) clearly indicates that fRe increases with increasing Reynolds number Re and surface relative roughness k/D_h because μ_R is proportional to Re and k/D_h. In addition, it is shown in Eq. (19) that for very small Re, the effect of surface roughness may be neglected, and fRe is approximately equal to the theoretical value of 67, which is supported by our experimental data. It can be seen from Fig. 5 that for $L^+ > 0.45$, the experimental results agree with the theoretical value well, and therefore, the present microchannels can be considered as smooth. On the other hand, we should note that the simplifying assumption is included in Eq. (19). Thus, it is not an appropriate equation to compute the friction factors but is useful for qualitative analysis.

Wu and Cheng [12] studied the effect of the surface roughness on the flow and heat transfer in trapezoidal silicon microchannels with the same geometric parameters. Although the tested microchannels are trapezoidal in shape, the constant of $C(\gamma)$ is also about 67 according to Morini [8] with the aspect ratios of 0.2532 and 0.2537. Thus, their experimental data can be compared with ours. The friction factors are presented in Fig. 6 versus Reynolds number. The most striking result seen in Fig. 6 is that the f–Re curves depart gradually from the conventional theory with increasing surface roughness and Reynolds number. In addition, based on

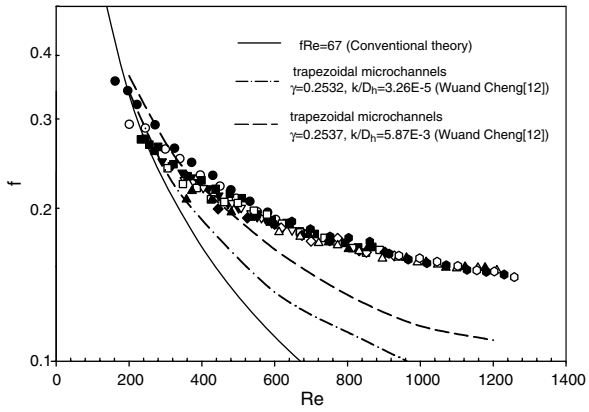

Fig. 6. The friction factors f versus the liquid Reynolds number Re.

the experimental data, the following correlation is proposed to predict the friction factors in rough rectangular microchannels for laminar flow.

$$f\,Re^{0.4743} = 4.0922 \tag{20}$$

The correlation of Eq. (20) is obtained using 140 data points. The maximum error is less than 2.84%.

It is known that the surface roughness does not influence the laminar flow in macrochannels. However, as seen in Figs. 5 and 6, such effect becomes important for laminar flow in microchannels due to the large surface to volume ratios.

4.2. Heat transfer

To determine the effect of thermally developing laminar flow in the entrance region, the non-dimensional axial distance for the thermal entrance region is defined as

$$X^+ = \frac{X}{D_h Re\, Pr} \tag{21}$$

$$L_h^+ = \frac{L}{D_h Re\, Pr} \tag{22}$$

where $X_1, X_2, \ldots, X_6$ correspond to the six thermocouple locations, respectively.

Correlations of the local Nusselt number for laminar flow in ducts are obtained using the solutions by Shah and London [13].

$$Nu_x = 8.24 - 16.8\gamma + 25.4\gamma^2 - 20.4\gamma^3 + 8.70\gamma^4, \quad X^+ \geqslant 0.1 \tag{23a}$$

$$Nu_x = 3.35(X^+)^{-0.130}\gamma^{-0.120}Pr^{-0.38}, \quad 0.013 \leqslant X^+ < 0.1 \tag{23b}$$

$$Nu_x = 1.87(X^+)^{-0.300}\gamma^{-0.056}Pr^{-0.036}, \quad 0.005 < X^+ < 0.013, \tag{23c}$$

The local Nusselt number Nu_x is plotted in Fig. 7 versus X^+ and compared with that of the conventional theory to identify the entrance effects on the local heat transfer. Fig. 7 corresponds to three different runs of $T_{in} = 30$ °C, $Q = 150$ W; $T_{in} = 70$ °C, $Q = 150$ W; and $T_{in} = 70$ °C, $Q = 350$ W. These curves clearly demonstrate that the Nu_x decreases with increasing X^+ at the locations of $X_2/L = 0.26$ and $X_3/L = 0.38$ due to the thermally developing flow. Furthermore, the Nu_x varies versus X^+ more rapidly for the run of $T_{in} = 30$ °C, $Q = 150$ W than those for the other two runs due to the higher Prandtl number at the lower heating power. However, the slope of the Nu_x against X^+ is quite gentle at the locations of $X_4/L = 0.62$ and $X_5/L = 0.74$, indicating that the thermally developed flow is approached at these locations. The higher Nusselt numbers at the location of $X_5/L = 0.74$ is due to the solid heat conduction effect because such location is quite close to the exit of the microchannels. Under such condition, the solid heat conduction causes the lower solid temperatures, and thus, higher Nusselt numbers can be obtained.

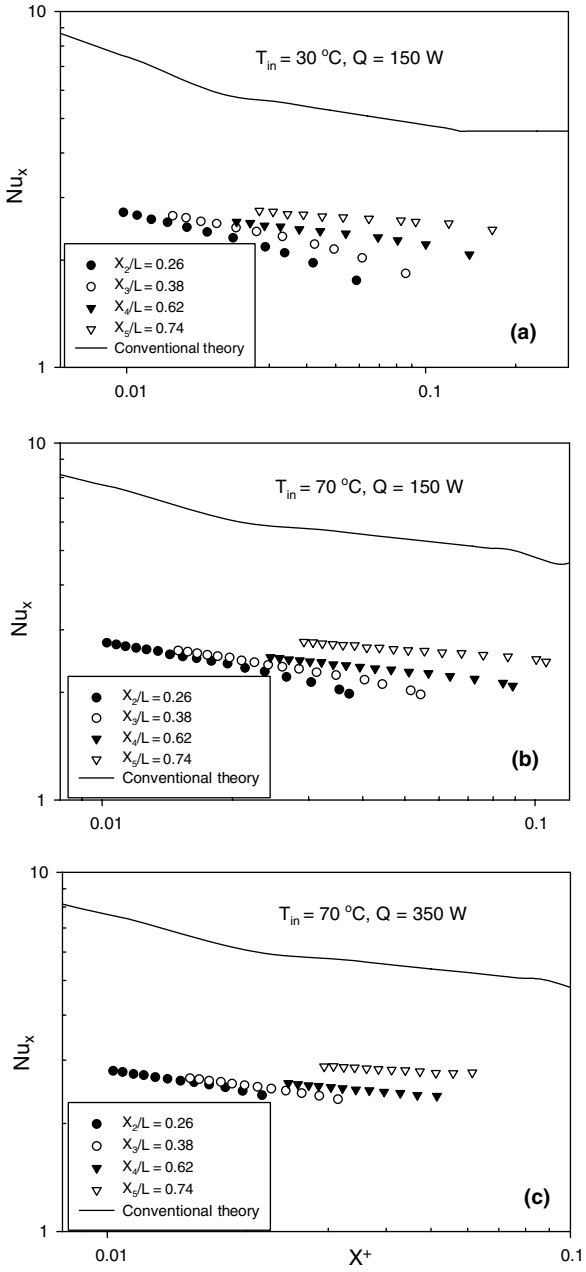

Fig. 7. The local Nusselt numbers Nu_x versus the non-dimensional thermal length X^+.

Fig. 8 shows the typical wall temperature T_w, fluid temperature T_f and heat transfer coefficient h distributions along the flow direction. The wall temperatures are computed from the measured temperatures. As seen from this figure, the locations at X_1 and X_2 in the entrance region have smaller temperature differences between the wall and the fluid, and thus, higher heat transfer coefficients are obtained, which are attributed to the thermally developing flow. From the locations X_2 to X_4, the linear distribution of the wall temperatures can be found, which is parallel to the linear liquid temperature distribution, causing the small heat transfer coefficient variation, as shown in Fig. 8b, indicating the thermally developed flow. Comparing the location at X_5 with other locations, a sudden increase of the heat transfer coefficients is found in Fig. 8b. This increasing trend is due to the heat conduction effects, which may slightly overestimate the heat transfer coefficients at

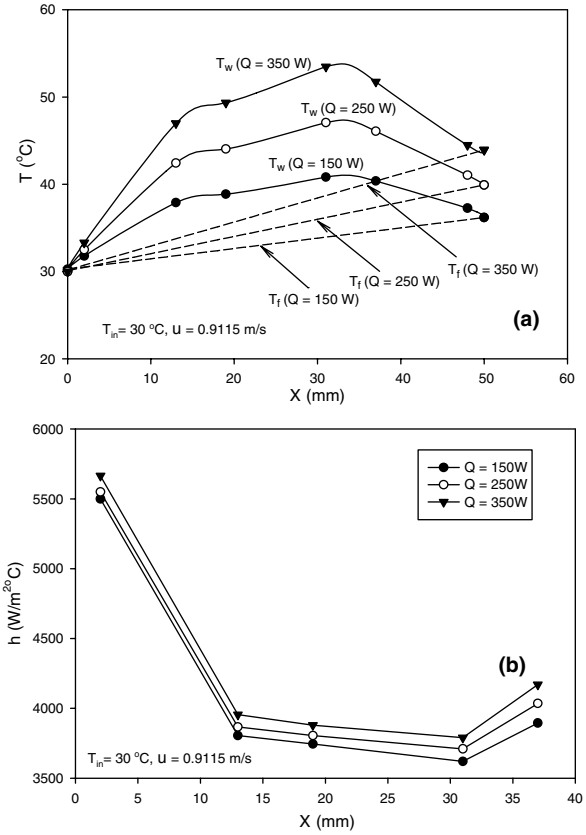

Fig. 8. The fluid temperature T_f, wall temperature T_w and heat transfer coefficient h along the flow direction.

the fifth location, X_5. From the above discussion, it is concluded that the measurements at X_1, X_2, X_3 and X_4 are nearly not affected by the heat conduction effects and can be used to determine the average heat transfer coefficients in the microchannels. The average Nusselt number Nu is given by the average of Nu_x at the first four locations of the microchannels.

$$Nu = (Nu_x(X_1) + Nu_x(X_2) + Nu_x(X_3) + Nu_x(X_4))/4 \tag{24}$$

The average Nusselt number Nu versus the non-dimensional channel heating length L_h^+ is plotted in Fig. 9. The $Nu - L_h^+$ curves exhibit two distinct regions. For small L_h^+, the average Nusselt numbers decrease rapidly with increasing L_h^+, indicating thermally developing flow in the microchannels for small L_h^+. The average Nusselt numbers become independent of L_h^+ when $L_h^+ > 0.14$, indicating thermally developed laminar flow in microchannels.

Considering the thermally developing flow in microchannels, the Nusselt numbers are correlated as follows:

$$Nu = 0.5046(PrRe)^{0.2221}, \quad 0.0375 < L_h^+ < 0.14 \tag{25a}$$

$$Nu = 2.181, \quad L_h^+ > 0.14 \tag{25b}$$

The correlation of Eq. (25a) uses 133 data points. The maximum error is less than 3.37%. The correlation of Eq. (25b) uses 7 data points, whose maximum error is less than 2.24%.

For the hydraulically developed but thermally developing flow in channels, the average Nusselt numbers for constant wall heat fluxes can be computed by Shah [14].

$$Nu = 1.953(RePrD_h/L)^{1/3}, \quad RePrD_h/L \geqslant 33.3 \tag{26a}$$

$$Nu = 4.364 + 0.0722RePrD_h/L, \quad RePrD_h/L \leqslant 33.3 \tag{26b}$$

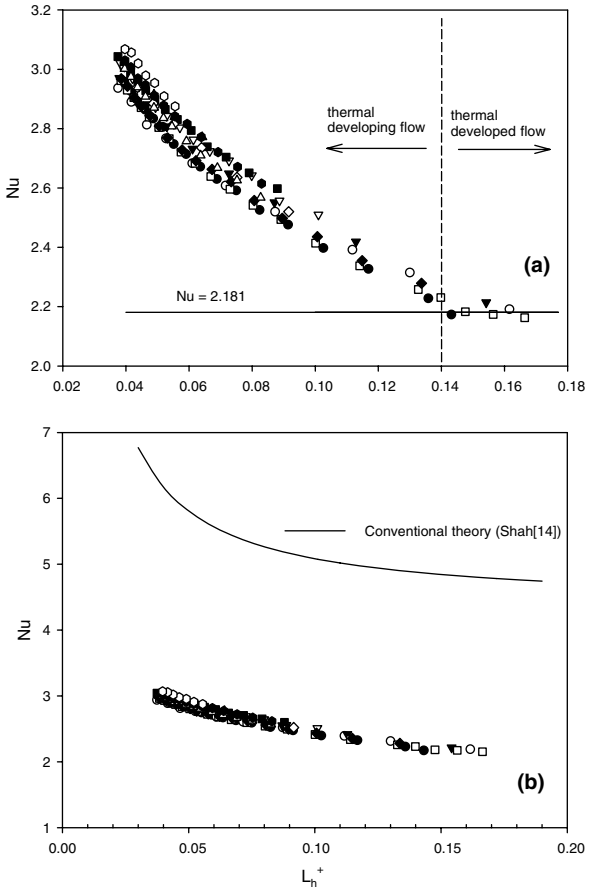

Fig. 9. The averaged Nusselt number Nu versus the non-dimensional thermal length L_h^+.

In Fig. 9b, the measured average Nusselt numbers are compared with the predictions using Eq. (26). The experimental data are found to be significantly lower than the conventional theory predictions. Similar results can also be seen in Fig. 7. The significant departure from conventional theory may be attributed to two main factors: the cross-sectional aspect ratio γ and the surface roughness k. Other factors such as the electrical double layer effect and the surface hydrophilic property are of secondary importance in the present study.

The previous studies show that the cross-sectional aspect ratio has a great influence on the heat transfer in microchannels [15,16]. It is found that even if the length to diameter ratio L/D_h and other parameters are identical, the Nusselt numbers in microchannels are quite different for different cross-sectional aspect ratios. Clearly, Eq. (26) neglect the effect of the aspect ratio. Therefore, conventional theory, such as Eq. (26), may not be applicable for heat transfer estimations in microchannels.

Qu et al. [5] studied the effect of surface roughness on the heat transfer coefficient in microchannels. They proposed a roughness-viscosity model to interpret their experimental data. On the basis of Merkle et al.'s [17] modified-viscosity model, Mala and Li [9] recommended a roughness-viscosity model that accounts for this additional momentum transfer by introducing a roughness viscosity μ_R. The apparent viscosity of the fluid μ_{app} is the sum of the fluid viscosity μ_f and the roughness viscosity μ_R. The velocity gradient near the wall surface is decreased due to the surface roughness effect. The fluid temperature gradient near the wall surface follows the same trend as the velocity, leading to decreased heat transfer coefficients. This may be another reason why the measured Nusselt numbers are significantly lower than the conventional theory predictions. They found that the predictions by the modified model agree with the experimental data well.

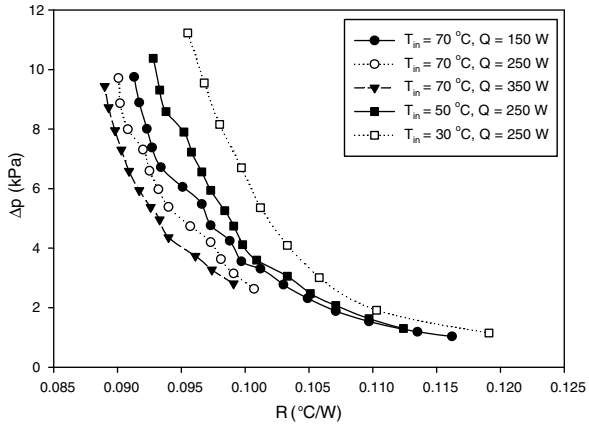

Fig. 10. The pressure drops Δp versus the thermal resistance R.

The pressure drops are plotted versus the thermal resistances in Fig. 10 for different inlet fluid temperatures and heating powers. Plotting pressure drop against thermal resistance is the best way to evaluate and compare thermal systems because they are competing factors considered in any practical thermo-hydraulic design. As seen in Fig. 10, the pressure drops in the microchannels decrease with increasing thermal resistance. In addition, the inlet fluid temperatures and the heating powers have a great effect on the R–Δp curves. For fixed thermal resistance, the pressure drop is smaller when the inlet fluid temperature or the heating power is higher, which may be attributed to the reduced fluid viscosities. Moreover, the combination of higher inlet fluid temperatures and heating powers yields lower pressure drops and thermal resistances.

5. Conclusion

The single phase convective heat transfer in rough copper rectangular microchannels is studied in this paper. The following conclusions can be obtained:

- The surface roughness has a great effect on the laminar flow in rough microchannels. For developed flow, the Poiseuille number in the regime of high Reynolds numbers is higher than the conventional theory predictions and increases with increasing Reynolds number, rather than remaining constant. However, such effect can be neglected for low Reynolds numbers.
- The average Nusselt number increases with increasing Reynolds number and Prandtl number. The trend is true for local Nusselt numbers also. The heat transfer enhancement is due to the thermally developing laminar flow. It is found that both the local and the average Nusselt numbers are significantly lower than the conventional theory predictions for all flow rates. This is attributed to two main factors: the cross-sectional aspect ratio and the surface roughness.
- Based on the present experimental data, correlations for friction factors and Nusselt numbers are obtained for deionized water flowing in rough rectangular microchannels with the surface relative roughness of 4–6%.
- The analysis shows that higher inlet fluid temperatures and heating powers can provide better overall flow and thermal performance.

Acknowledgments

This work is supported by the National Natural Science Foundation of China (50476088), the Natural Science Foundation of Guangdong Province (32700) and the Science and Technology Development Foundation of Guangdong Province (33103).

References

[1] Wu P, Little WA. Measurement of friction factors for the flow of gases in very fine channels used for microminiature Joule–Thomson refrigerators. Cryogenics 1983;23:273–7.
[2] Wu P, Little WA. Measurement of the heat transfer characteristics of gas flow in very fine channels used for microminiature refrigerators. Cryogenics 1984;24:415–20.
[3] Kandlikar SG, Joshi S, Tian S. Effect of channel roughness on heat transfer and fluid flow characteristics at low Reynolds numbers in small diameter tubes. In: Proc of 35th national heat transfer conference, Anaheim CA, USA, 2001, paper 12134.
[4] Qu W, Mala GM, Li D. Pressure-driven water flows in trapezoidal silicon microchannels. Int J Heat Mass Transfer 2000;43:353–64.
[5] Qu W, Mala GM, Li D. Heat transfer for water flow in trapezoidal silicon microchannels. Int J Heat Mass Transfer 2000;43:3925–36.
[6] Kays WM, London AL. Compact heat exchangers. New York: McGraw-Hill; 1984.
[7] Harms TM, Kazmierczak MJ, Gerner FM. Developing convective heat transfer in deep rectangular microchannels. Int J Heat Fluid Flow 1999;20:149–57.
[8] Morini GL. Laminar-to-turbulent flow transition in microchannels. Microscale Thermophys Eng 2004;8:15–30.
[9] Mala GM, Li D. Flow characteristics of water in microtubes. Int J Heat Fluid Flow 1999;20:142–8.
[10] Potter MC, Wiggert DC. Mechanics of fluids. 2nd ed. Prentice Hall Inc; 1997.
[11] Gao P, Le Person S, Favre-Marinet M. Scale effects on hydrodynamics and heat transfer in two-dimensional mini and microchannels. Int J Therm Sci 2002;41:1017–27.
[12] Wu HY, Cheng P. An experimental study of convective heat transfer in silicon microchannels with different surface conditions. Int J Heat Mass Transfer 2003;46:2547–56.
[13] Shah RK, London AL. Advances in heat transfer. Supplement 1: laminar flow forced convection in ducts. New York: Academic Press; 1978.
[14] Shah RK. Thermal entry length solutions for the circular tube and parallel plates. In: Proc 3rd national heat mass transfer conference, Indian Inst Technol Bombay, vol. I, 1975, paper HMT-11-75.
[15] Wu HY, Cheng P. Friction factors in smooth trapezoidal silicon microchannels with different aspect ratios. Int J Heat Mass Transfer 2003;46:2519–25.
[16] Peng XF, Peterson GP. Convective heat transfer and flow friction for water flow in microchannel structures. Int J Heat Mass Transfer 1996;39:2599–608.
[17] Merkle CL, Kubota T, Ko DRS. An analytical study of the effects of surface roughness on boundary-layer transition. AF Office of Scien Res Space and Missile Sys Org AD/A004786, 1974.